 doi:10.20944/preprints202102.0467.v1

Article

Vegetation Structure Index (VSI): Retrieving Vegetation Structural Information from Multi-angular Satellite Remote Sensing

Ram C. Sharma

Department of Informatics, Tokyo University of Information Sciences, 4-1 Onaridai, Wakaba-ku, Chiba 265-8501, Japan; sharma@rsch.tuis.ac.jp

* Correspondence: sharma@rsch.tuis.ac.jp; Tel./Fax: +81-43-236-1408

Abstract: Utilization of Bidirectional Reflectance Distribution Function (BRDF) model parameters obtained from the multi-angular remote sensing is one of the approaches for the retrieval of vegetation structural information. In this research, the potential of multi-angular vegetation indices, formulated by the combination of multi-spectral reflectance from different view angles, for the retrieval of forest above ground biomass was assessed. This research was implemented in the New England region with the availability of a high quality forest inventory database. The multi-angular vegetation indices were generated by the simulation of the Moderate Resolution Imaging Spectroradiometer (MODIS) BRDF/Albedo Model Parameters Product (MCD43A1 Version 6) based BRDF parameters. The effects of seasonal (spring, summer, autumn, and winter) composites of the multi-angular vegetation indices on above ground biomass, angular relationship of the spectral reflectance with above ground biomass, and the interrelationships between the multi-angular vegetation indices were analyzed. Among the existing multi-angular vegetation indices, only the Nadir BRDF-adjusted NDVI ($\mathrm{NDVI_{iso}}$) and Hot-spot incorporated NDVI ($\mathrm{NDVI_{HS}}$) showed significant relationship (more than 50%) with the above ground biomass. This research proposed two more sensitive vegetation structural indices, Fore-scattering Back-scattering NDVI and Vegetation Structure Index (VSI). The Fore-scattering Back-scattering NDVI showed higher sensitivity ($R^2 = 0.62$, RMSE = 52.46) towards the above ground biomass than existing multi-angular vegetation indices. Furthermore, the VSI performed in the most efficient way explaining 64% variation of the above ground biomass, suggesting that the right choice of the spectral channel and observation geometry should be considered for improving the estimates of the above ground biomass. In addition, the right choice of seasonal data (summer) was found to be important for estimating the forest biomass while other seasonal data were either insensitive or pointless. The promising results shown by the VSI suggest that it could be an appropriate candidate for monitoring vegetation structure from the multi-angular satellite remote sensing.

Keywords: Forests, Structure, Biomass, BRDF, MODIS, Multi-angular, NDVI (Fore-Back), Vegetation structure index

---

1. Introduction

Forests have experienced dramatic changes in terms of cover, density, and biomass worldwide. Monitoring of forest biomass and carbon stocks changes is vital to comprehend deforestation and degradation conditions that have implications for the climate system. At local scales, forest structural parameters such as diameter at breast height, canopy height, etc. can be obtained from the measurement of individual trees. Then, the forest biomass can be estimated with allometric functions which provides a functional relationship with easily measured variables such as standing tree height and diameter at breast height (Jenkins et al., 2004; Chave et al., 2004). However, satellite remote sensing is an expected technology for upscaling the in situ estimates of forest biomass into broad scales.

Preprints (www.preprints.org) | NOT PEER-REVIEWED | Posted: 22 February 2021 doi:10.20944/preprints202102.0467.v1

One of the approaches for the retrieval of forest structural information from the remote sensing imagery is the utilization of bidirectional reflectance distribution function (BRDF) model parameters obtained from the multi-angular observations. The multi-angular remote sensing has also been utilized for characterization of biomes (Bacour et al., 2005), forests (Rautiainen et al., 2008), agricultural landscape (Román et al., 20111), vegetation physiognomic types (Sharma and Hara, 2018), and chemical attributes of the canopy (Song et al., 2016; Liu and Liu, 2018).

The anisotropic reflectance property of the land surface, i.e., directional dependency of the reflectance with sun-sensor geometry, has long been studied (Kimes, 1986; Li and Strahler 1992; Sandmeier and Deering, 1999; Gerard and North, 1997). Researchers have developed some BRDF models such as computer simulation (North, 1996), empirical (Walthall et al., 1997), physical radiative transfer (Verhoef, 1984; Verstraete et al., 1990; Liang and Strahler, 1994), physical geometric optical (Li and Strahler, 1985, 1992; Jupp and Strahler, 1991), and semi-emperical (Lavergne et al., 2007; Roujean et al., 1992) to describe the anisotropic characteristics of the land surface. These BRDF models have many applications such as normalizing the BRDF effects of images taken at multiple sun-sensor geometry, estimation of albedo by integration of multi-angular reflectance, and retrieval of land surface attributes by the interpretation of BRDF shapes (Lucht, 2000; Jiao, 2009; Liu et al., 2009; Gao, 2003; Pinty et al., 2002).

The Ross-Thick Li-Sparse-Reciprocal (RTLSR) is one of the semi-empirical BRDF models. In this model, the bi-directional reflectance (R) is described for a given sun zenith angle (SZA), view zenith angle (VZA), and relative azimuth angle (RAA) as shown by Equation 1 (Li and Strahler, 1985; Roujean et al., 1992; Wanner et al., 1995; Lucht et al., 2000).

$$R(\theta,\vartheta,\Delta\phi) = f_{iso} + f_{vol} \times K_{vol}\,(\theta,\vartheta,\Delta\phi) + f_{geo} \times K_{geo}\left(\theta,\vartheta,\Delta\phi,\tfrac{h}{b},\tfrac{b}{r}\right) \qquad (1)$$

In Equation (1), K_{vol} *and* K_{geo} are the kernels for volumetric scattering and geometric scattering respectively. The K_{vol} *and* K_{geo} are trigonometric functions of SZA (θ), VZA (ϑ), and RAA ($\Delta\phi$); crown relative height $\left(\frac{h}{b}\right)$ and relative shape $\left(\frac{b}{r}\right)$ parameters are also included in K_{geo}. The f_{iso}, f_{vol} *and* f_{geo} are the constraint isotropic, volumetric and geometric scattering respectively. Full derivation of the RossThick and the LiSparse kernels are described in Wanner et al. (1995).

For the retrieval of forest biophysical parameters from the multi-angular remote sensing, different approaches such as radiative transfer modeling (North, 1996), geometric-optical modeling (Chopping et al., 2011), spectral invariant (Schull et al., 2011; Lewis et al., 2007) and BRDF model parameters (d'Entremont et al., 1999; Doll et al., 2001; Gao et al., 2003) have been attempted by the researchers. Another approach for the retrieval of forest structural information is the utilization of multi-angular vegetation indices which are formulated by the combination of spectral reflectance measured from multiple view angles. An overview of the multi-angular indices available in the literature has been presented in Table 1.

Table 1. Overview of the multi-angular vegetation indices available in the literature.

Multi-angular vegetation indices	Formula	Reference	Target areas
Nadir BRDF-adjusted NDVI ($NDVI_{iso}$)	$\frac{Nir_{0,0,0} - Red_{0,0,0}}{Nir_{0,0,0} + Red_{0,0,0}}$	Schaaf et al., 2002	Vegetation parameters
Anisotropy index ($ANIX_{Red}$)	$\frac{H_{red}}{D_{red}}$	Sandmeier et al., 1998	Land cover types
Anisotropy index ($ANIX_{Nir}$)	$\frac{H_{nir}}{D_{nir}}$	Sandmeier et al., 1998	Land cover types
Hot-spot dark spot index (HDS_{red})	$\frac{\mathrm{H_{red}} - \mathrm{D_{red}}}{\mathrm{D_{red}}}$	Lacaze et al., 2002	Vegetation clumping
Normalized difference between hot-spot and dark-spot index ($NDHD_{nir}$)	$\frac{\mathrm{H_{nir}} - \mathrm{D_{nir}}}{\mathrm{H_{nir}} + \mathrm{D_{nir}}}$	Chen et al., 2005	Vegetation clumping
Hot-spot dark-spot NDVI ($\mathrm{NDVI_{HD}}$)	$\frac{\mathrm{H_{nir}} - \mathrm{D_{red}}}{\mathrm{H_{nir}} + \mathrm{D_{red}}}$	Pocewicz et al., 2007	Leaf area index
Hot-spot incorporated NDVI ($\mathrm{NDVI_{HS}}$)	$N_{\mathrm{NDVI}} \times (1 - \mathrm{H_{red}})$	Pocewicz et al., 2007	Leaf area index

Preprints (www.preprints.org) | NOT PEER-REVIEWED | Posted: 22 February 2021 doi:10.20944/preprints202102.0467.v1

The major objective of this research is to assess the potential of multi-angular vegetation indices for the retrieval of forest above ground biomass. This research also proposes more sensitive vegetation indices to the above ground biomass. The effects of seasonal composites of the multi-angular vegetation indices on above ground biomass, angular relationship of the spectral reflectance with above ground biomass, and the interrelationships between the multi-angular vegetation indices have also been discussed.

2. Materials and Methods

2.1. Study areas

This research was implemented in the New England region where a high quality forest inventory database has been available freely (Cook et al., 2011). The database constitutes the field measurements conducted in five forests in 2009. The size of sample plots were 1 ha. The description of the study sites, consisting of geo-locations, forest types, and major species have been shown in Table 2.

Table 2. Description of the study sites (Cook et al., 2011).

Study sites	Geo-locations	Forest types	Major species
Harvard Forest, Massachusetts	42.53°, -72.17°	Moist temperate	Red oak, red maple, yellow birch, white birch, black birch, beech, white pine, eastern hemlock
Howland Research Forest, Maine	45.20°, -68.73°	Mature evergreen	Red spruce, eastern hemlock, balsam fir, white pine, northern white cedar
Hubbard Brook Experimental Forest, New Hampshire	43.56°, -71.45°	Deciduous hardwoods	Sugar maple, beech, yellow birch, white ash
Bartlett Experimental Forest, New Hampshire	44.04°, -71.16°	Deciduous hardwoods	Beech, yellow birch, sugar maple, eastern hemlock, red maple, paper birch, aspen, red spruce, white pine
Penobscott Experimental Forest, Maine	44.86°, -68.65°	Mixed conifers and hardwoods	Eastern hemlock, spruce, red, white, balsam fir, northern white cedar, eastern white pine, tamarack, red pine, red maple, paper birch, gray birch, aspen

2.2. In situ biomass estimates

The above ground biomass were calculated with diameter at breast height greater than 10 cm using the allometric function (Jenkins et al., 2004) shown by (Equation 2). In Equation 2, the above ground biomass (B) in kg was calculated by the exponential function of diameter at breast height (dbh) in cm. The species-specific parameters, a and b were varied from -0.712 to -2.54 and 1.7 to 2.48 respectively.

$$B = exp^{a + (b \times \ln(dbh))} \quad (2)$$

The sample plots nearby heterogeneous land cover types such as built-up areas and water ponds were discarded for the analysis. In this manner, among 59 sample plots available, 55 sample plots were selected for this research. In five forests, the above ground biomass ranged from 18.72 to 330.29 Mg/ha with mean value of 188.19 Mg/ha which was considered quite diverse for the assessment of multi-angular vegetation indices. Location map of the study sites and distribution of sample plots have been shown in Figure 1.

Preprints (www.preprints.org) | NOT PEER-REVIEWED | Posted: 22 February 2021 doi:10.20944/preprints202102.0467.v1

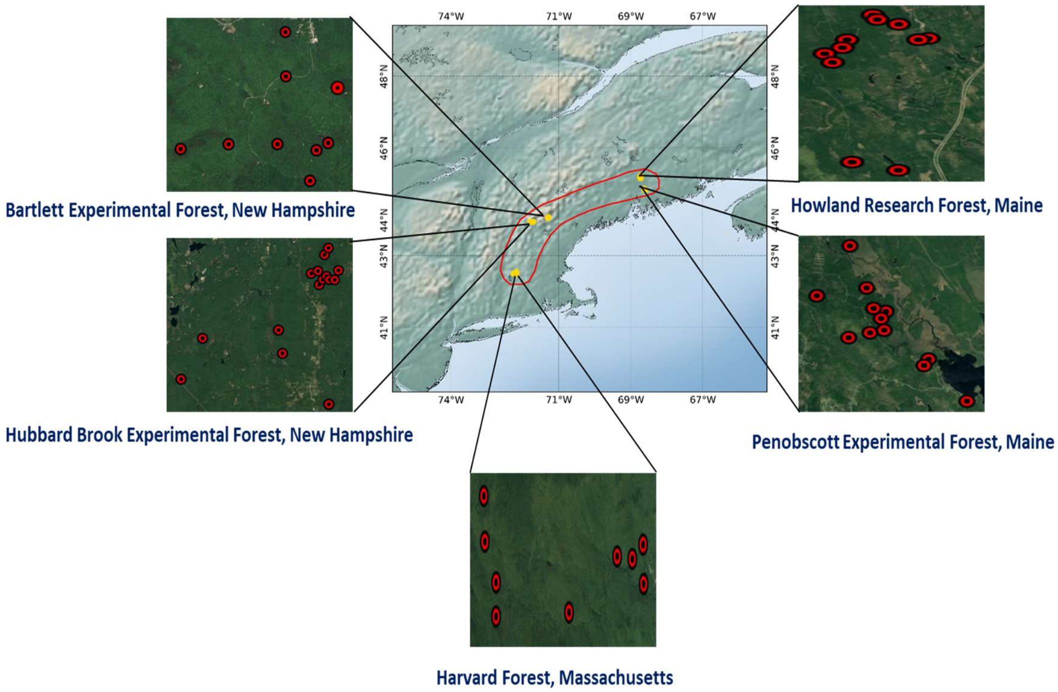

Figure 1. Location of the study sites and distribution of the sample plots.

2.3. Proposal of new multi-angular indices

A typical forest canopy is composed of green canopy cover (sunlit crown and shadowed crown) and canopy shadow fraction (shadowed ground and shadowed crown). The fractional area of the canopy components vary significantly in the principal plane with respect to the view zenith angles (Sharma et al., 2013). While the scene viewed from the Back-scattering direction (45, 45, 0) is mostly composed of sunlit ground and sunlit crown, the shadowed crown and shadowed ground dominate the scene viewed from the Fore-scattering direction (45, 45, 180). Red reflectance at the Back-scattering direction is sensitive to hiding of the ground which should be faster in tall and dense (high-biomass) canopy. Larger the ground surface hidden by canopies, lower the red reflectance at the Back-scattering direction. On the other hand, near infrared reflectance at the Fore-scattering direction is sensitive to the canopy shadows which should be higher in short and sparse (low-biomass) canopy. Lower the canopy shadows and open ground exposed in the Fore-scattering direction, higher the near-infrared reflectance at the Fore-scattering direction. Therefore, Fore-scattering (Fore) and Back-scattering (Back) Normalized Difference Vegetation Index (NDVI) has been proposed as the normalized difference between the Near Infrared (Nir) reflectance observed at Fore-scattering (Fore) direction and the Red reflectance (Red) observed at Back-scattering (Back) direction (Equation 3) to be sensitive to the volumetric structure of the forest canopy.

$$NDVI_{Fore-bac} = \frac{Nir_{Fore} - Red_{Back}}{Nir_{Fore} + Red_{Back}} \tag{3}$$

Furthermore, the Vegetation Structure Index (VSI) has been proposed by integrating the non-linear interaction of the vegetation coverage ratio, indicated by the term $(1 - Nir_{Fore})$ with the $NDVI_{Fore-bac}$ (Equation 4).

$$VSI = \frac{NDVI_{Fore-back}}{1 - Nir_{Fore}} \tag{4}$$

2.4. Processing of satellite data

The Moderate Resolution Imaging Spectroradiometer (MODIS) BRDF/Albedo Model Parameters Product (MCD43A1) has been providing BRDF model parameters based on the RTLSR model (Schaaf et al., 2002). The BRDF model parameters (f_{iso}, f_{vol} and f_{geo}) were obtained from the

 doi:10.20944/preprints202102.0467.v1

MODIS BRDF/Albedo product (MCD43A1 Version 6) of 2009. This dataset is produced daily using 16 days of Terra and Aqua MODIS data at 500 meter (m) resolution (Schaaf et al., 2002). Using the central geolocation point of each plot, BRDF model parameters were extracted for a single MODIS pixel. Then, the bidirectional reflectance for the assumed Hot-spot (45, 45, 0), Nadir (45, 0, 0), and Dark-spot (45, 45, 180) were calculated by using the BRDF model parameters (f_{iso}, f_{vol} and f_{geo}) and look up values (K_{vol} and K_{geo}). The Back-scattering and Fore-scattering reflectance were obtained from the assumed Hot-spot (45, 45, 0) and Dark-spot (45, 45, 180) geometries respectively. Seasonal median composites, spring (March - May), summer (June - August), autumn (September - November), and winter (December - February), were generated from the daily calculations of the multi-angular vegetation indices.

3. Results and Discussion

3.1. Performance of existing multi-angular indices

The performance of the multi-angular vegetation indices was assessed using linear regression analysis with the in situ above ground biomass data in terms of Coefficient of determination (R^2) and Root Mean Square Error (RMSE). The relationships between existing multi-angular spectral indices and above ground biomass have been shown in Figure 2, and the results have also been summarized in Table 3.

Preprints (www.preprints.org) | NOT PEER-REVIEWED | Posted: 22 February 2021 doi:10.20944/preprints202102.0467.v1

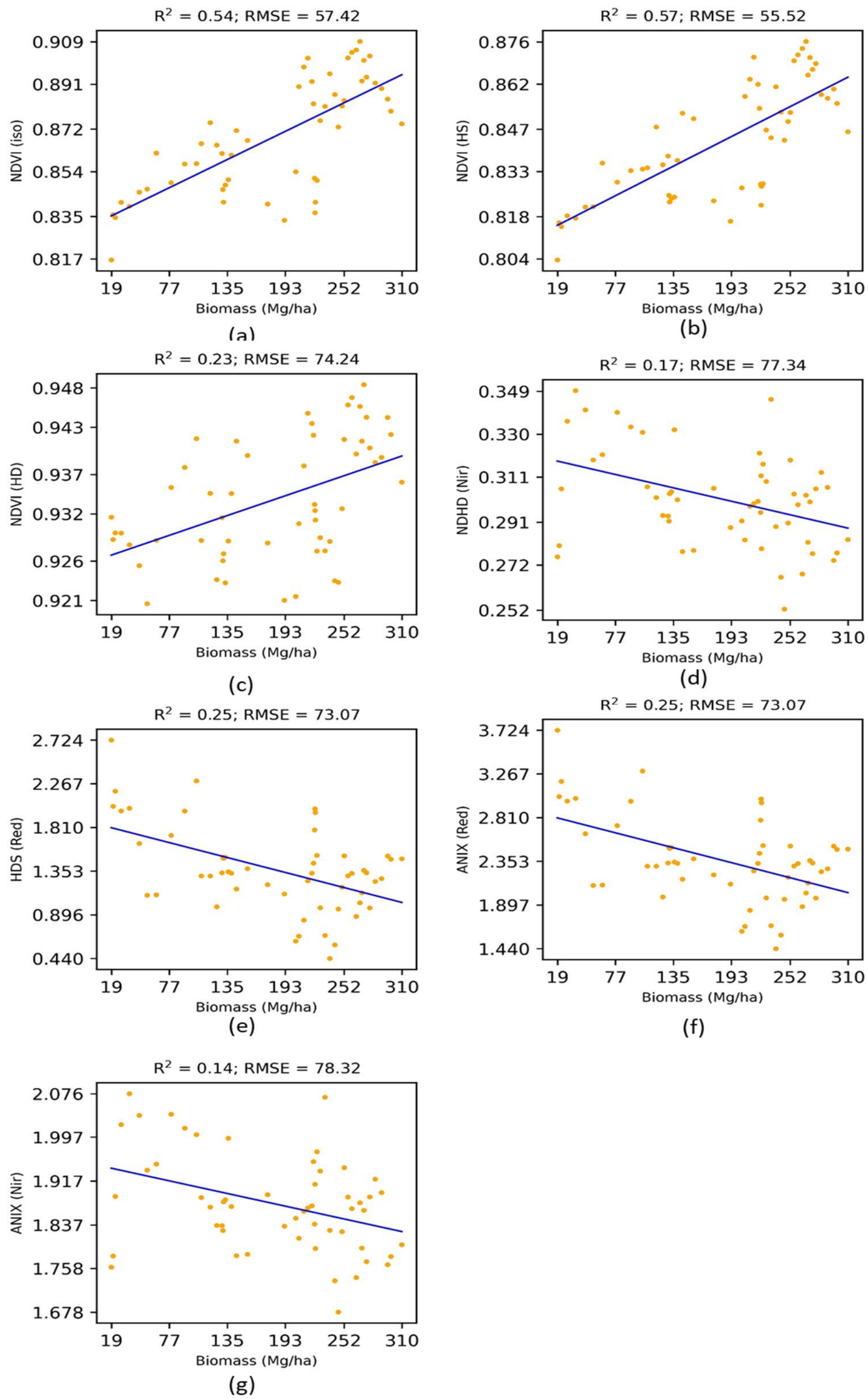

Figure 2. Performance of existing multi-angular vegetation indices for the estimation of above ground biomass.

Preprints (www.preprints.org) | NOT PEER-REVIEWED | Posted: 22 February 2021 doi:10.20944/preprints202102.0467.v1

Table 3. Performance of existing multi-angular vegetation indices.

Multi-angular vegetation indices	R^2	RMSE
Anisotropy index ($ANIX_{Red}$)	0.25	73.07
Anisotropy index ($ANIX_{Nir}$)	0.14	78.32
Hot-spot dark spot index (HDS_{red})	0.25	73.07
Normalized difference between hot-spot and dark-spot index ($NDHD_{nir}$)	0.17	77.34
Hot-spot dark-spot NDVI ($\mathrm{NDVI_{HD}}$)	0.23	74.24
Hot-spot incorporated NDVI ($\mathrm{NDVI_{HS}}$)	0.57	55.52
Nadir BRDF-adjusted NDVI ($NDVI_{iso}$)	0.54	57.42

As shown in Table 3, only the Nadir BRDF-adjusted NDVI ($NDVI_{iso}$) and Hot-spot incorporated NDVI ($NDVI_{HS}$) showed significant relationship (more than 50%) with the above ground biomass. Other multi-angular vegetation indices, Anisotropy index ($ANIX_{Red}$), Anisotropy index ($ANIX_{Nir}$), Hot-spot dark spot index (HDS_{red}), Normalized difference between hot-spot and dark-spot index ($NDHD_{nir}$), and Hot-spot dark-spot NDVI ($\mathrm{NDVI_{HD}}$) did not show sensitivity towards the above ground biomass.

3.2. Performance of new multi-angular indices

The $NDVI_{Fore-back}$ showed higher sensitivity (R^2 = 0.62, RMSE = 52.46) towards the above ground biomass than existing multi-angular vegetation indices (Table 3). Furthermore, the Vegetation Structure Index (VSI) proposed in the research performed in the most efficient way explaining 64% variation of the above ground biomass (Figure 3).

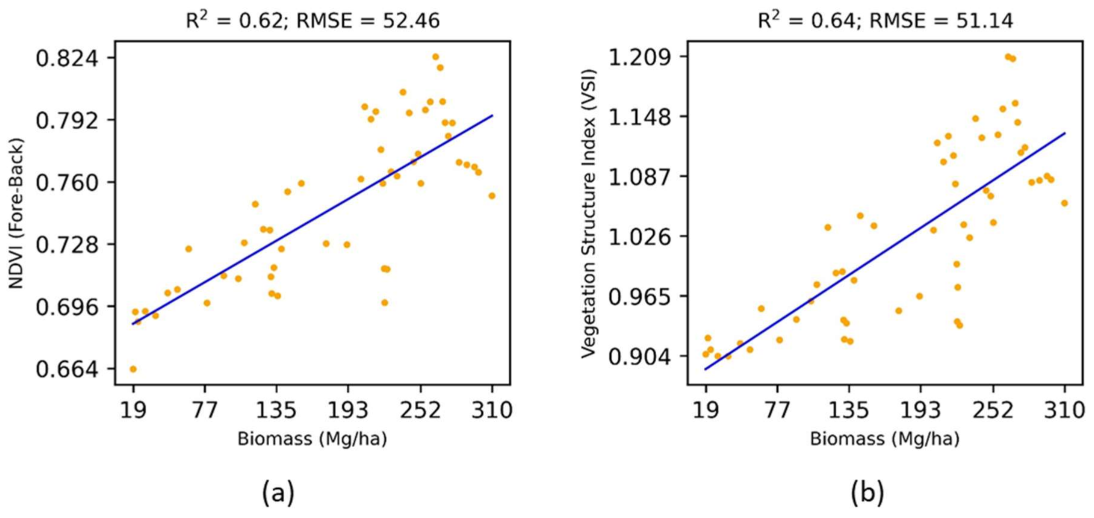

Figure 3. Performance of new multi-angular vegetation indices for the estimation of above ground biomass.

3.3. Effects of view angles on biomass

The effects of the view angles (Fore-scattering versus Dark-scattering) on the above ground biomass has been shown in Figure 4.

doi:10.20944/preprints202102.0467.v1

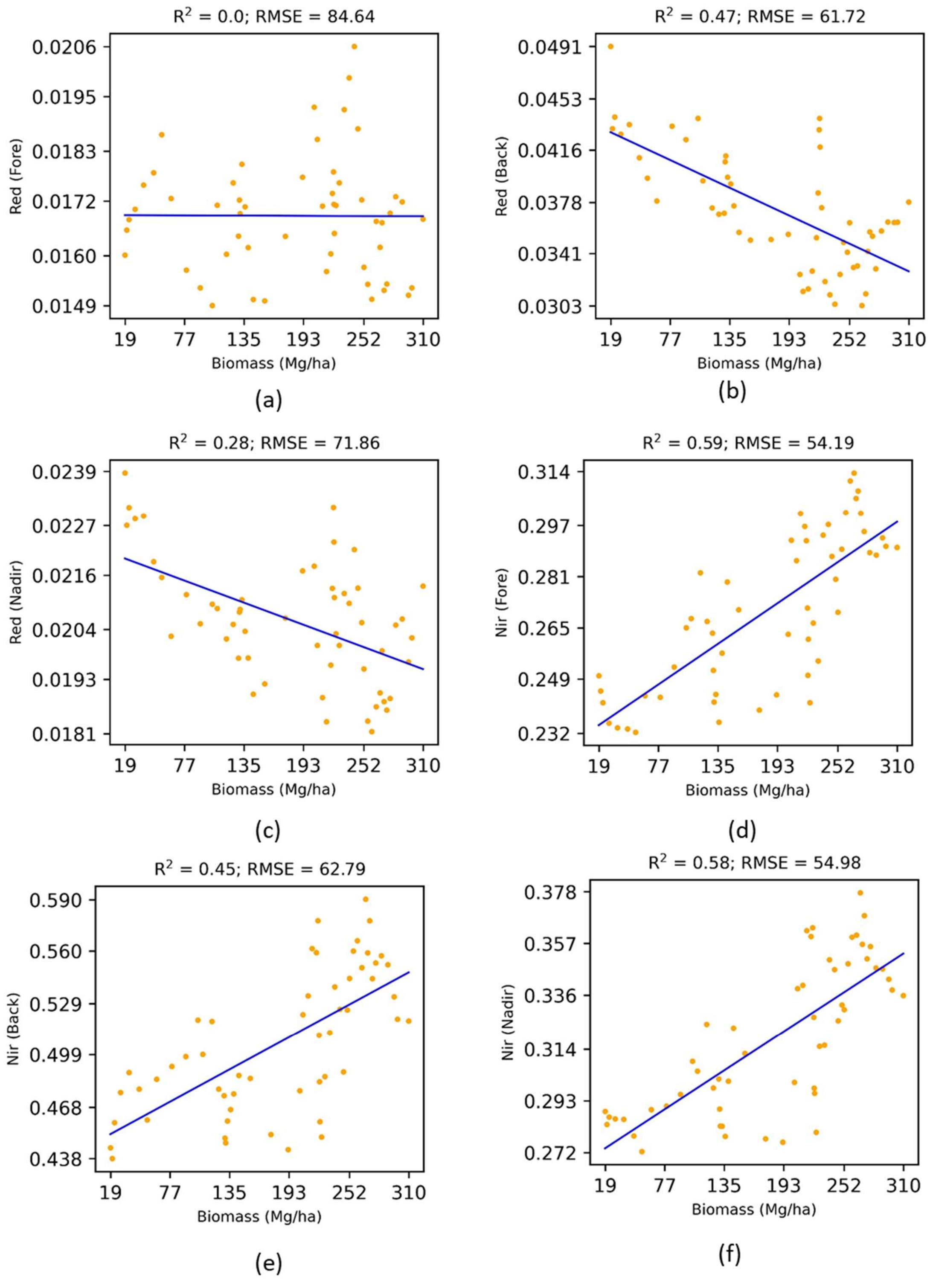

Figure 4. Effects of view angles on the above ground biomass.

For the Red reflectance, the Back-scattering direction was found to be more sensitive to the above ground biomass than the Nadir direction; whereas Fore-scattering direction was quite insensitive. Both the Back-scattering and Nadir reflectance were inversely proportional to the above ground biomass. In contrast, for the Near Infrared reflectance, the Fore-scattering direction was found to be more sensitive to the above ground biomass than the Back-scattering and Nadir directions. All three

 doi:10.20944/preprints202102.0467.v1

directions (Fore-scattering, Back-scattering, and Nadir) were directly proportional to the above ground biomass. Therefore, the right choice of the spectral channel and observation geometry should be considered for improving the estimates of above ground biomass. It should be noted that the NDVI (Fore-Back) has been built by integrating the most sensitive spectral channel and observation geometry.

3.4. Interrelationships between structural indices

Figure 5 shows the interrelationships between multi-angular structural indices. NDVI (Fore-Back) was more related to the NDVI (iso) than the NDVI (HD). Nevertheless, NDVI (Fore-Back) and NDVI (HD) were quite distinct with lower coefficient of determinitation (R^2= 0.27). The relationship bettween VSI and NDVI (iso) was lower (R^2= 0.88) than that of NDVI (Fore-Back) and NDVI (iso). Still, the newly proposed indices in the research are quite distint from the existing indices while being more sensitive towards the above ground biomass.

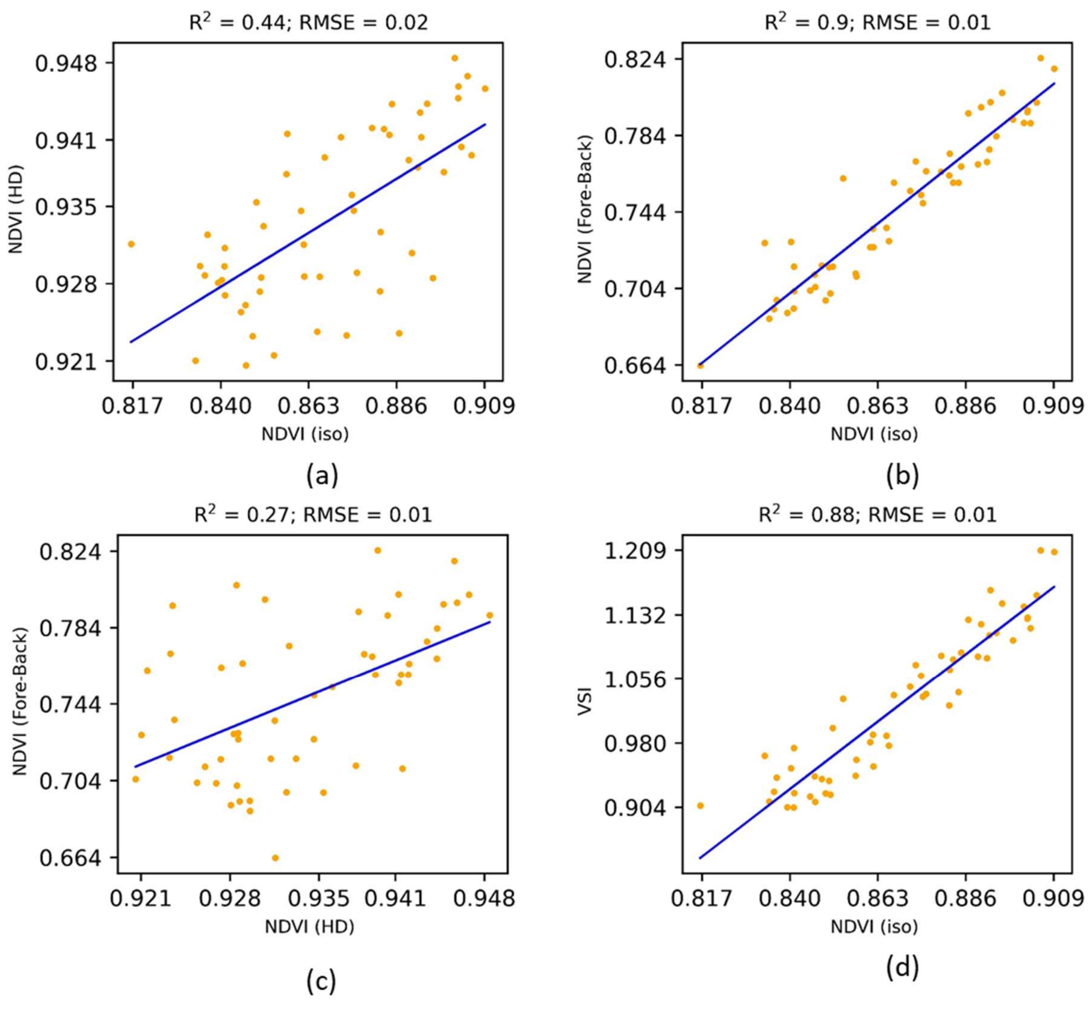

Figure 5. Interrelationships between multi-angular indices.

3.5. Effects of seasonal data on biomass

The analysis on above sections (3.1 to 3.4) were based on median composites of the reflectance in the summer season. Figures 6 and 7 show the seasonal effects of multi-angular vegetation indices (NDVI-iso and VSI) on the above ground biomass. Both the NDVI-iso and VSI in summer were most

Preprints (www.preprints.org) | NOT PEER-REVIEWED | Posted: 22 February 2021 doi:10.20944/preprints202102.0467.v1

sensitive to the above ground biomass; whereas other seasons were either insensitive (winter season) or pointless (spring and autumn seasons with a decreasing trend). Therefore, the right choice of seasonal data was found to be important for estimating the forest biomass.

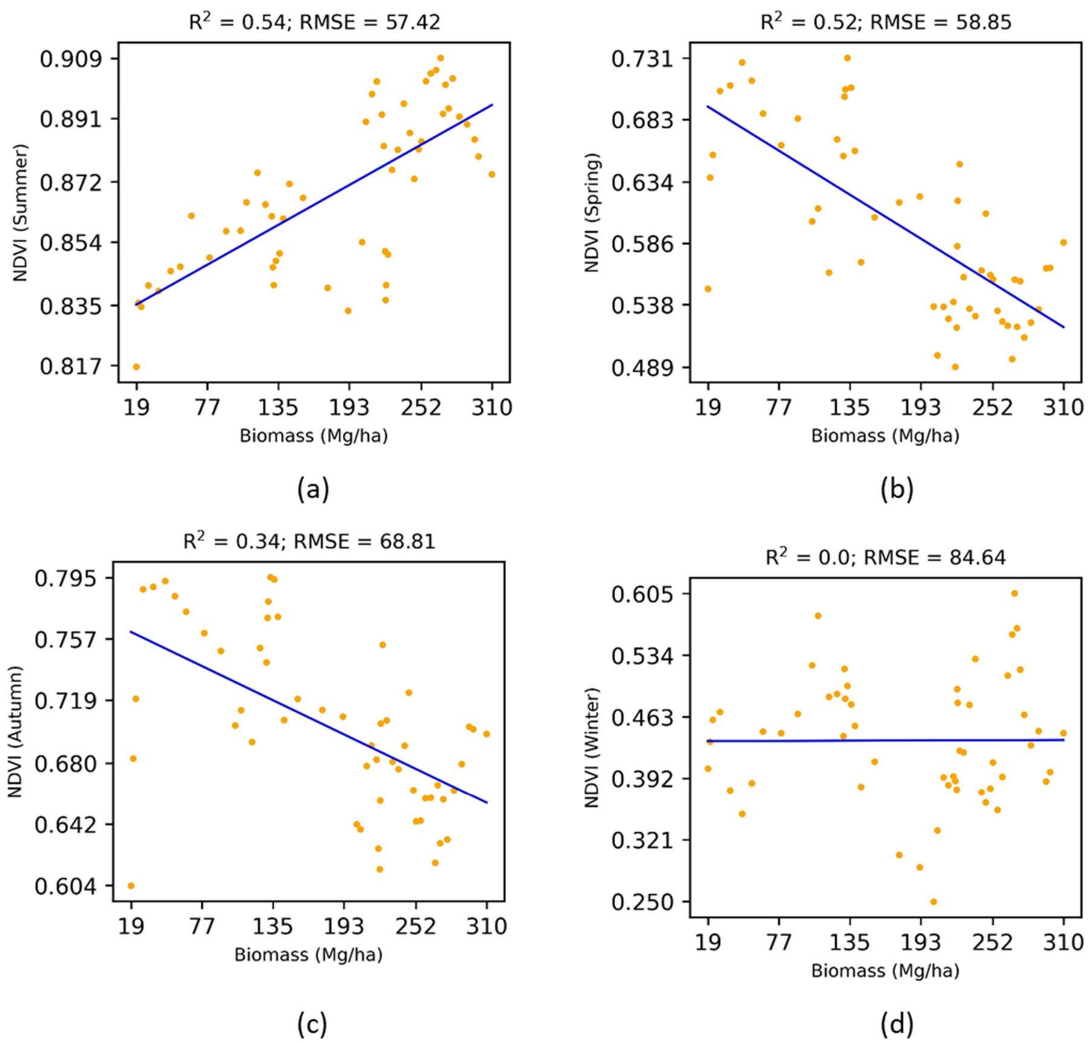

Figure 6. Effects of seasonal NDVI (iso) on the above ground biomass.

 doi:10.20944/preprints202102.0467.v1

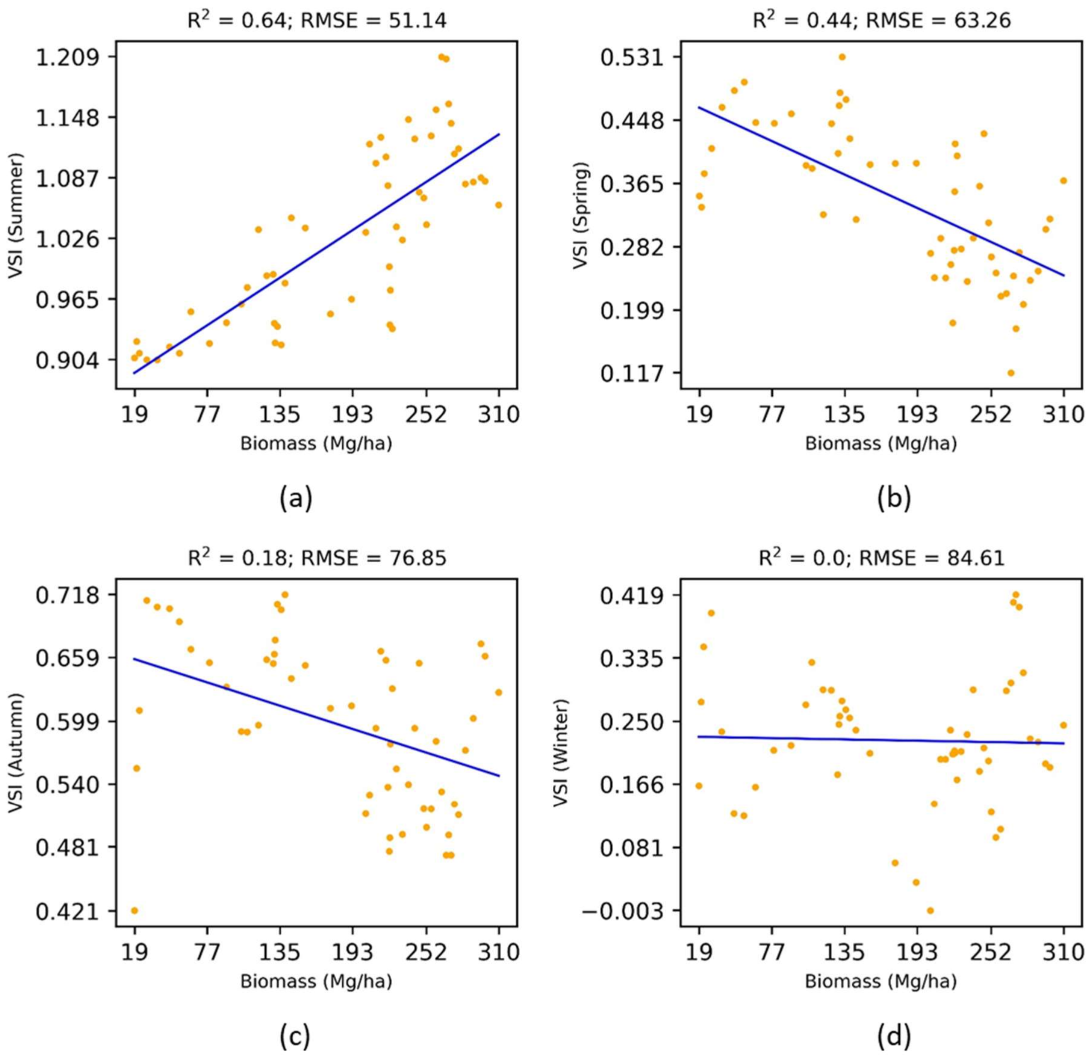

Figure 7. Effects of seasonal VSI on the above ground biomass.

5. Conclusion

Derivation of more sensitive vegetation indices from multi-angular remote sensing data is important for better retrieval of the vegetation structural information. In this research, The $NDVI_{Fore-back}$ has been proposed on the concept that higher Near Infrared reflectance at the Fore-scattering direction indicates exposure of higher contents of the canopy volume, whereas lower Red reflectance at the Back-scattering direction indicates suppression of the ground reflectance with higher contents of the canopy volume. Furthermore, the Vegetation Structure Index (VSI) has been proposed by integrating the non-linear interaction of the vegetation coverage ratio, indicated by the term $(1 - Nir_{Fore})$ with the $NDVI_{Fore-back}$. In this research, the VSI was found to be more sensitive to the above ground biomass in the New England forests than other extant multi-angular vegetation indices. It suggests that the right choice of the spectral channel and observation geometry should be considered for improving the estimates of the above ground biomass. In addition, the right choice of seasonal data (summer) was found to be important for estimating the forest biomass while other seasonal data were either insensitive or pointless. The VSI has been derived from the MODIS based BRDF parameters which can be generated all over the globe. Availability of much higher resolution bi-directional reflectance data is expected in the future for improved estimates of the above ground biomass in the field of multi-angular satellite remote sensing.

Acknowledgments: MODIS data used in the research were available from the NASA EOSDIS Land Processes Distributed Active Archive Center (LP DAAC).

Funding: This research received no funding.

References

1. Bacour, C.; Bréon, F.-M. Variability of Biome Reflectance Directional Signatures as Seen by POLDER. *Remote Sensing of Environment* **2005**, *98*, 80–95, doi:10.1016/j.rse.2005.06.008.
2. Chave, J.; Condit, R.; Aguilar, S.; Hernandez, A.; Lao, S.; Perez, R. Error Propagation and Scaling for Tropical Forest Biomass Estimates. *Philosophical Transactions of the Royal Society of London. Series B: Biological Sciences* **2004**, *359*, 409–420, doi:10.1098/rstb.2003.1425.
3. Chen, J.M.; Menges, C.H.; Leblanc, S.G. Global Mapping of Foliage Clumping Index Using Multi-Angular Satellite Data. *Remote Sensing of Environment* **2005**, *97*, 447–457, doi:10.1016/j.rse.2005.05.003.
4. Chopping, M.; Schaaf, C.B.; Zhao, F.; Wang, Z.; Nolin, A.W.; Moisen, G.G.; Martonchik, J.V.; Bull, M. Forest Structure and Aboveground Biomass in the Southwestern United States from MODIS and MISR. *Remote Sensing of Environment* **2011**, *115*, 2943–2953, doi:10.1016/j.rse.2010.08.031.
5. Cook, B.; Dubayah, R.; Griffith, P.; Hall, F.G.; Nelson, R.; Ranson, J.; Simard, M.; Siqueira, P.; Strahler, A.H. NACP NEW ENGLAND AND SIERRA NATIONAL FORESTS BIOPHYSICAL MEASUREMENTS: 2008-2010 2011.
6. d'Entremont, R.P.; Schaaf, C.B.; Lucht, W.; Strahler, A.H. Retrieval of Red Spectral Albedo and Bidirectional Reflectance Using AVHRR HRPT and GOES Satellite Observations of the New England Region. *Journal of Geophysical Research: Atmospheres* **1999**, *104*, 6229–6239, doi:10.1029/1998JD200104.
7. Doll, C.N.H.; Muller, J.-P.; Schaaf, C.; Strahler, A.H.; Feng Gao Mapping Urban Landcover Using the Bidirectional Reflectance Distribution Function BRDF/Albedo Product from the Moderate Resolution Imaging Spectroradiometer (MODIS). In Proceedings of the IGARSS 2001. Scanning the Present and Resolving the Future. Proceedings. IEEE 2001 International Geoscience and Remote Sensing Symposium (Cat. No.01CH37217); IEEE: Sydney, NSW, Australia, 2001; Vol. 6, pp. 2680–2682.
8. Gao, F. Detecting Vegetation Structure Using a Kernel-Based BRDF Model. *Remote Sensing of Environment* **2003**, *86*, 198–205, doi:10.1016/S0034-4257(03)00100-7.
9. Gerard, F.F.; North, P.R.J. Analyzing the Effect of Structural Variability and Canopy Gaps on Forest BRDF Using a Geometric-Optical Model. *Remote Sensing of Environment* **1997**, *62*, 46–62, doi:10.1016/S0034-4257(97)00070-9.
10. Jenkins, J.C.; Chojnacky, D.C.; Heath, L.S.; Birdsey, R.A. Comprehensive Database of Diameter-Based Biomass Regressions for North American Tree Species. *Gen. Tech. Rep. NE-319. Newtown Square, PA: US Department of Agriculture, Forest Service, Northeastern Research Station. 45 p.[1 CD-ROM].* **2004**, *319*.
11. Jupp, D.L.B.; Strahler, A.H. A Hotspot Model for Leaf Canopies. *Remote Sensing of Environment* **1991**, *38*, 193–210, doi:10.1016/0034-4257(91)90089-O.
12. Kimes, D.S.; Newcomb, W.W.; Nelson, R.F.; Schutt, J.B. Directional Reflectance Distributions of a Hardwood and Pine Forest Canopy. *IEEE Transactions on Geoscience and Remote Sensing* **1986**, *GE-24*, 281–293, doi:10.1109/TGRS.1986.289647.
13. Lacaze, R. Retrieval of Vegetation Clumping Index Using Hot Spot Signatures Measured by POLDER Instrument. *Remote Sensing of Environment* **2002**, *79*, 84–95, doi:10.1016/S0034-4257(01)00241-3.
14. Lavergne, T.; Kaminski, T.; Pinty, B.; Taberner, M.; Gobron, N.; Verstraete, M.M.; Vossbeck, M.; Widlowski, J.-L.; Giering, R. Application to MISR Land Products of an RPV Model Inversion Package Using Adjoint and Hessian Codes. *Remote Sensing of Environment* **2007**, *107*, 362–375, doi:10.1016/j.rse.2006.05.021.
15. Lewis, P.; Disney, M. Spectral Invariants and Scattering across Multiple Scales from Within-

Leaf to Canopy. *Remote Sensing of Environment* **2007**, *109*, 196–206, doi:10.1016/j.rse.2006.12.015.
16. Li, X.; Strahler, A. Geometric-Optical Modeling of a Conifer Forest Canopy. *IEEE Transactions on Geoscience and Remote Sensing* **1985**, *GE-23*, 705–721, doi:10.1109/TGRS.1985.289389.
17. Li, X.; Strahler, A.H. Geometric-Optical Bidirectional Reflectance Modeling of the Discrete Crown Vegetation Canopy: Effect of Crown Shape and Mutual Shadowing. *IEEE Transactions on Geoscience and Remote Sensing* **1992**, *30*, 276–292, doi:10.1109/36.134078.
18. Liang, S.; Strahler, A. Retrieval of Surface BRDF from Multiangle Remotely Sensed Data. *Remote Sensing of Environment* **1994**, *50*, 18–30, doi:10.1016/0034-4257(94)90091-4.
19. Liu, X.; Liu, L. Influence of the Canopy BRDF Characteristics and Illumination Conditions on the Retrieval of Solar-Induced Chlorophyll Fluorescence. *International Journal of Remote Sensing* **2018**, *39*, 1782–1799, doi:10.1080/01431161.2017.1404165.
20. Lucht, W.; Schaaf, C.B.; Strahler, A.H. An Algorithm for the Retrieval of Albedo from Space Using Semiempirical BRDF Models. *IEEE Transactions on Geoscience and Remote Sensing* **2000**, *38*, 977–998, doi:10.1109/36.841980.
21. North, P.R.J. Three-Dimensional Forest Light Interaction Model Using a Monte Carlo Method. *IEEE Transactions on Geoscience and Remote Sensing* **1996**, *34*, 946–956, doi:10.1109/36.508411.
22. Pocewicz, A.; Vierling, L.A.; Lentile, L.B.; Smith, R. View Angle Effects on Relationships between MISR Vegetation Indices and Leaf Area Index in a Recently Burned Ponderosa Pine Forest. *Remote Sensing of Environment* **2007**, *107*, 322–333, doi:10.1016/j.rse.2006.06.019.
23. Rautiainen, M.; Lang, M.; Mõttus, M.; Kuusk, A.; Nilson, T.; Kuusk, J.; Lükk, T. Multi-Angular Reflectance Properties of a Hemiboreal Forest: An Analysis Using CHRIS PROBA Data. *Remote Sensing of Environment* **2008**, *112*, 2627–2642, doi:10.1016/j.rse.2007.12.005.
24. Román, M.O.; Gatebe, C.K.; Schaaf, C.B.; Poudyal, R.; Wang, Z.; King, M.D. Variability in Surface BRDF at Different Spatial Scales (30m–500m) over a Mixed Agricultural Landscape as Retrieved from Airborne and Satellite Spectral Measurements. *Remote Sensing of Environment* **2011**, *115*, 2184–2203, doi:10.1016/j.rse.2011.04.012.
25. Roujean, J.-L.; Leroy, M.; Deschamps, P.-Y. A Bidirectional Reflectance Model of the Earth's Surface for the Correction of Remote Sensing Data. *Journal of Geophysical Research* **1992**, *97*, 20455, doi:10.1029/92JD01411.
26. Sandmeier, St.; Deering, D.W. Structure Analysis and Classification of Boreal Forests Using Airborne Hyperspectral BRDF Data from ASAS. *Remote Sensing of Environment* **1999**, *69*, 281–295, doi:10.1016/S0034-4257(99)00032-2.
27. Sandmeier, St.; Müller, Ch.; Hosgood, B.; Andreoli, G. Physical Mechanisms in Hyperspectral BRDF Data of Grass and Watercress. *Remote Sensing of Environment* **1998**, *66*, 222–233, doi:10.1016/S0034-4257(98)00060-1.
28. Schaaf, C.B.; Gao, F.; Strahler, A.H.; Lucht, W.; Li, X.; Tsang, T.; Strugnell, N.C.; Zhang, X.; Jin, Y.; Muller, J.-P.; et al. First Operational BRDF, Albedo Nadir Reflectance Products from MODIS. *Remote Sensing of Environment* **2002**, *83*, 135–148, doi:10.1016/S0034-4257(02)00091-3.
29. Schull, M.A.; Knyazikhin, Y.; Xu, L.; Samanta, A.; Carmona, P.L.; Lepine, L.; Jenkins, J.P.; Ganguly, S.; Myneni, R.B. Canopy Spectral Invariants, Part 2: Application to Classification of Forest Types from Hyperspectral Data. *Journal of Quantitative Spectroscopy and Radiative Transfer* **2011**, *112*, 736–750, doi:10.1016/j.jqsrt.2010.06.004.
30. Sharma, R.; Hara, K. Characterization of Vegetation Physiognomic Types Using Bidirectional Reflectance Data. *Geosciences* **2018**, *8*, 394, doi:10.3390/geosciences8110394.
31. Sharma, R.C.; Kajiwara, K.; Honda, Y. Estimation of Forest Canopy Structural Parameters Using Kernel-Driven Bi-Directional Reflectance Model Based Multi-Angular Vegetation Indices. *ISPRS Journal of Photogrammetry and Remote Sensing* **2013**, *78*, 50–57, doi:10.1016/j.isprsjprs.2012.12.006.
32. Song, X.; Feng, W.; He, L.; Xu, D.; Zhang, H.-Y.; Li, X.; Wang, Z.-J.; Coburn, C.A.; Wang, C.-Y.; Guo, T.-C. Examining View Angle Effects on Leaf N Estimation in Wheat Using Field Reflectance Spectroscopy. *ISPRS Journal of Photogrammetry and Remote Sensing* **2016**, *122*, 57–67, doi:10.1016/j.isprsjprs.2016.10.002.

33. Walthall, C. A Study of Reflectance Anisotropy and Canopy Structure Using a Simple Empirical Model. *Remote Sensing of Environment* **1997**, *61*, 118–128, doi:10.1016/S0034-4257(96)00245-3.
34. Wanner, W.; Li, X.; Strahler, A.H. On the Derivation of Kernels for Kernel-Driven Models of Bidirectional Reflectance. *Journal of Geophysical Research* **1995**, *100*, 21077, doi:10.1029/95JD02371.